Catalysis Today 175 (2011) 18–25

Contents lists available at ScienceDirect

Catalysis Today

journal homepage: www.elsevier.com/locate/cattod

Mechanism of the selective catalytic reduction of NO_x with NH_3 over environmental-friendly iron titanate catalyst

Fudong Liu, Hong He*, Changbin Zhang, Wenpo Shan, Xiaoyan Shi

State Key Laboratory of Environmental Chemistry and Ecotoxicology, Research Center for Eco-Environmental Sciences, Chinese Academy of Sciences, Beijing 100085, PR China

ARTICLE INFO

Article history:
Received 22 October 2010
Received in revised form 25 January 2011
Accepted 26 February 2011
Available online 1 April 2011

Keywords:
Selective catalytic reduction
Iron titanate catalyst
Langmuir–Hinshelwood mechanism
Eley–Rideal mechanism
Rate-determining step

ABSTRACT

The reaction mechanism of the selective catalytic reduction (SCR) of NO_x with NH_3 over environmental-friendly iron titanate catalyst ($FeTiO_x$) was investigated in detail. Over the iron titanate crystallite with specific Fe–O–Ti structure, both Brønsted and Lewis acid sites were present and involved in the SCR reaction. NH_3 mainly adsorbed on titanium sites in the form of ionic NH_4^+ and coordinated NH_3, while NO_x mainly adsorbed on iron sites in the form of monodentate nitrate. In a relatively low temperature range (<200 °C), the SCR process mainly followed the Langmuir–Hinshelwood (L–H) mechanism, in which the formation of monodentate nitrate from NO oxidation by O_2 over Fe^{3+} was the rate-determining step. In contrast, in a relatively high temperature range (>200 °C), the SCR process mainly followed the Eley-Rideal (E–R) mechanism, in which the formation of NH_2NO intermediate species following the H-abstraction of NH_3 by neighboring Fe^{3+} was the rate-determining step.

1. Introduction

Nitrogen oxides (NO_x) producing from stationary and mobile sources, such as coal-fired power plants and diesel engines, have been a major air pollutant deteriorating the atmospheric environment. To meet more and more stringent environmental standards established worldwide for NO_x emission control, selective catalytic reduction (SCR) of NO_x over catalytic materials with various reducing agents (such as ammonia, urea, hydrocarbons, *etc.*) has been well studied. NH_3-SCR is a well-proven and effective technology for the elimination of NO_x from stationary sources, which has been industrially utilized since 1970s. Besides, it is also one of the most promising technologies for the removal of NO_x from diesel engines. For NH_3-SCR process, the most widely used catalyst system is V_2O_5–WO_3 (MoO_3)/TiO_2, in which the active phase V_2O_5 is yet biologically toxic. Nowadays, many researchers are focusing on the development of new environmental-friendly NH_3-SCR catalysts to substitute the conventional vanadium-based catalyst, which also shows some other problems in practical use, such as narrow operation temperature window, low N_2 selectivity and high conversion of SO_2 to SO_3 at high temperatures. In our previous works [1–4], we have successfully developed a novel and environmental-friendly iron titanate catalyst ($FeTiO_x$) with specific Fe–O–Ti structure, showing excellent NH_3-SCR activity, N_2 selectivity and H_2O/SO_2 durability in the medium temperature range (200–400 °C). However, the SCR mechanism over this catalyst is still unclear.

Even for V_2O_5–WO_3 (MoO_3)/TiO_2 catalyst, which has been used for decades, several debates in mechanistic aspects still remain, such as the intrinsic nature of active sites [5] and reactive adsorbed NH_3 species (bound to Brønsted or Lewis acid sites) involved in the SCR reaction [6]. Similarly, different SCR mechanisms have been proposed over Fe-based catalysts, including Langmuir–Hinshelwood (L–H) mechanism and Eley–Rideal (E–R) mechanism. Over Fe^{3+}–TiO_2–PILC catalyst prepared by Long and Yang [6], they proposed that both ionic NH_4^+ and coordinated NH_3 could react with adsorbed NO_2 to form intermediate species, which could further react with NO to form N_2 and H_2O, following an L–H mechanism. Whereas, over Fe–ZSM-5 catalyst prepared by Long and Yang [7], it was proposed that only ionic NH_4^+ contributed to the SCR reaction, following a similar L–H mechanism. Contrastively, Apostolescu et al. pointed out that over Fe_2O_3–WO_3/ZrO_2 catalyst the SCR reaction mainly followed an E–R mechanism, in which only Lewis acid sites were involved in NH_3 activation and NO reduction process [8]. Therefore, the SCR mechanisms proposed by researchers over different catalysts are usually diverse. It is necessary to get a comprehensive understanding of the reac-

* Corresponding author at: Research Center for Eco-Environmental Sciences, State Key Laboratory of Environmental Chemistry and Ecotoxicology, P.O. Box 2871, 18 Shuangqing Road, Haidian District, Beijing 100085, PR China. Tel.: +86 10 62849123; fax: +86 10 62849123.
E-mail address: honghe@rcees.ac.cn (H. He).

0920-5861/$ – see front matter © 2011 Elsevier B.V. All rights reserved.
doi:10.1016/j.cattod.2011.02.049

tion mechanism over $FeTiO_x$ catalyst synthesized by our group for further improving its low temperature SCR activity and H_2O/SO_2 durability for industrial application.

In this article, temperature programmed desorption (TPD), temperature programmed surface reaction (TPSR), transient response (TR) and *in situ* diffuse reflectance infrared Fourier transform spectroscopy (*in situ* DRIFTS) will be used for NH_3-SCR mechanism study over $FeTiO_x$ catalyst. The reactive surface species including adsorbed NH_3 and NO_x species will be clearly clarified. Two different mechanisms in the relatively low and high temperature ranges will be proposed accordingly, which can supply theoretical guidance for the catalyst redesign and thus the activity improvement.

2. Experimental

2.1. Catalyst preparation, SCR activity and characterizations

$FeTiO_x$ catalyst and Fe_2O_3, TiO_2 reference samples were prepared by co-precipitation method using $Fe(NO_3)_3{\cdot}9H_2O$ and $Ti(SO_4)_2$ as precursors [2]. During the preparation process of $FeTiO_x$ catalyst, $Ti(SO_4)_2$ and $Fe(NO_3)_3{\cdot}9H_2O$ were firstly dissolved together with distilled water with the molar ratio of Fe:Ti = 1:1. Afterwards, standard $NH_3{\cdot}H_2O$ (25 wt.%) was used as precipitator until the pH rose to 10 when the Fe and Ti ions were completely co-precipitated. Without aging, the precipitate was filtrated and washed, followed by desiccation at 100 °C for 12 h and calcination at 400 °C for 6 h in air condition. The calcined sample was crushed and sieved to 20–40 mesh for activity test and TPD, TPSR and TR experiments, and above 120 mesh for *in situ* DRIFTS experiments. As for reference samples, Fe_2O_3 and TiO_2 were self-prepared by precipitation method using $Fe(NO_3)_3{\cdot}9H_2O$ and $Ti(SO_4)_2$ as precursors, respectively. The desiccation, calcination and sieving procedures were controlled exactly the same as those of $FeTiO_x$ catalyst.

Our previous study [2] showed that $FeTiO_x$ catalyst showed a good NH_3-SCR activity in the temperature range of 200–350 °C with the NO_x conversion above 90%, which was 50-150 °C lower than those of Fe/ZSM-5 [9], Fe–TiO_2–PILC [10], $Fe_2O_3/WO_3/ZrO_2$ [8] and Fe/HBEA catalysts [11]. Based on the calculation results of turn-over frequency (TOF), the intrinsic activity of $FeTiO_x$ catalyst was also comparable to that of the state-of-the-art SCR catalyst V_2O_5–WO_3/TiO_2 or commercial Fe-exchanged BEA catalyst [11], but still much lower than that of Fe/ZSM-5 or Cu/ZSM-5 reported by other researchers [12,13] probably because this $FeTiO_x$ catalyst possessed a majority of ineffective iron species in the bulk phase. According to the XRD, UV–Vis DRS, Raman spectroscopy and XAFS results, the $FeTiO_x$ catalyst was mainly in the form of iron titanate crystallite with specific Fe–O–Ti structure, while the reference samples Fe_2O_3 and TiO_2 were mainly present as well-crystallized hematite and anatase, respectively [2]. The BET surface areas of $FeTiO_x$, Fe_2O_3 and TiO_2 obtained from N_2 physisorption results were 245.3, 42.5 and 103.5 m^2/g, respectively, and the BJH desorption pore volumes were 0.52, 0.21 and 0.20 $cm^3\ g^{-1}$, respectively [2].

2.2. TPD, TPSR and TR experiments

TPD, TPSR and TR experiments were performed over 200 mg samples in a fixed-bed quartz tube reactor using a quadrupole mass spectrometer (HPR20, Hiden Analytical Ltd., Amplifier Head HAL 301) to record the reactant signals. The recorded signals were as follows: m/z = 16 (NH_2) or 15 (NH) to identify NH_3 in the absence or presence of O_2; m/z = 30 to identify NO or NO_2; m/z = 18, 28, 32 and 44 to identify H_2O, N_2, O_2 and N_2O, respectively. Due to the very small relevant abundance of H_2O signal with m/z = 16 (*ca.* 0.9% comparing with m/z = 18 obtained from NIST Mass Spectrometry Data Center), we can distinguish NH_3 and H_2O species in mass spectrometer clearly.

Prior to the TPD, TPSR and TR experiments, the samples were pretreated in a flow of 20 vol% O_2/He (30 ml/min) at 300 °C for 30 min. After cooling down to room temperature, the O_2/He flow was switched to a flow of 2500 ppm NH_3/Ar or 2500 ppm NO + 10 vol% O_2/Ar (30 ml/min) for 1 h. Then the samples were purged with Ar for another 1 h until the mass spectrometer signals were stabilized. For TPD experiments, the temperature was directly raised linearly to 500 °C at a rate of 10 °C/min in a flow of Ar.

For TPSR experiments between adsorbed NH_3 species with NO or NO + O_2, subsequent to the NH_3 adsorption and Ar purge, the Ar flow was switched to different flows of 500 ppm NO/Ar or 500 ppm NO + 5 vol% O_2/Ar for 1 h until the concentrations of reactants were stabilized. Then the temperature was raised linearly to 500 °C at a rate of 10 °C/min. On the contrary, for TPSR experiment between adsorbed NO_x species with NH_3, subsequent to the NO + O_2 adsorption and Ar purge, the Ar flow was switched to a flow of 500 ppm NH_3/Ar for 1 h until the concentration of NH_3 was stabilized. Then the temperature was also raised linearly to 500 °C at a rate of 10 °C/min.

For TR experiments, subsequent to the NH_3 or NO + O_2 adsorption and Ar purge at room temperature, the temperature was raised to 200 °C or 150 °C and held on for 1 h until the partial desorption of surface species at this temperature was complete. Then NO + O_2 or NH_3 was turned on and off repeatedly to observe the pulse reaction between the gaseous reactants with adsorbed species. For TR experiments at 150 °C, Amplifier Head HAL 201 equipped on HPR20 mass spectrometer was used.

2.3. In situ DRIFTS

The *in situ* DRIFTS experiments were performed on an FTIR spectrometer (Nicolet Nexus 670) equipped with an MCT/A detector cooled by liquid nitrogen. An *in situ* reactor cell with ZnSe window (Nexus Smart Collector) connected to an adsorption/purging gas control system was used. The reaction temperature was controlled precisely by an Omega programmable temperature controller. Prior to each *in situ* DRIFTS experiment, the sample was pretreated at 400 °C in a flow of 20 vol% O_2/N_2 for 30 min and then cooled down to the desired reaction temperature (200 °C). The spectrum of $FeTiO_x$ catalyst at 200 °C was collected in flowing N_2 atmosphere and set as background, which was automatically subtracted from the final spectrum. The total flow rate of the feeding gas was kept at 300 ml/min and all spectra were recorded by accumulating 100 scans with a resolution of 4 cm^{-1}. The reaction conditions were controlled as follows: 500 ppm NO, 500 ppm NH_3, 5 vol% O_2 and N_2 balance.

3. Results

3.1. NH_3-TPD and NO_x-TPD experiments

The adsorption/desorption capacity of NH_3 and NO_x over $FeTiO_x$ catalyst was investigated by TPD methods using TiO_2 and Fe_2O_3 as reference samples (Fig. 1). As the NH_3-TPD results shown in Fig. 1A, all of the samples had three NH_3 desorption peaks from 30 to 500 °C. The peaks below 100 °C can be ascribed to physisorbed NH_3, and the peaks located at 100–120 °C can be ascribed to NH_4^+ bound to weak Brønsted acid sites (some surface hydroxyls) [14,15]. For $FeTiO_x$ and TiO_2, the desorption peaks above 200 °C can be ascribed to NH_4^+ bound to strong Brønsted acid sites (some surface hydroxyls with enhanced acidity induced by sulfate species and hydroxyls directly linked to sulfate species) and coordinated NH_3 bound

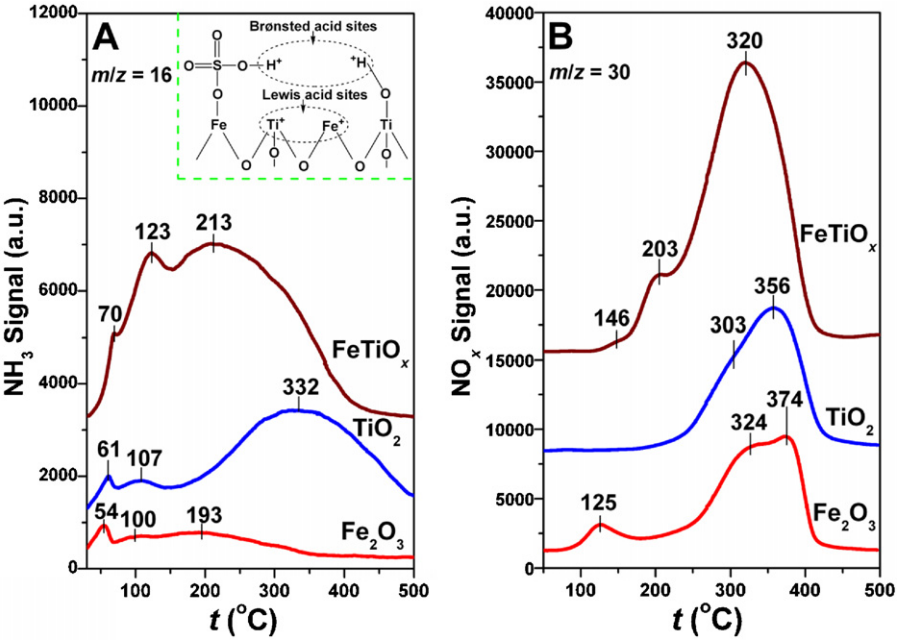

Fig. 1. (A) NH_3-TPD and (B) NO_x-TPD profiles over $FeTiO_x$, TiO_2 and Fe_2O_3.

to Lewis acid sites [16]. For Fe_2O_3, a lower and broader desorption peak was observed centered at 193 °C, which can be only attributed to NH_3 bound to Lewis acid sites because no sulfate species thus no strong Brønsted acid sites existed on this sample. In the whole temperature range, $FeTiO_x$ catalyst showed the maximum NH_3 adsorption and consequently desorption amount. The calculated NH_3 adsorption amounts on these three samples decreased in the following sequence: $FeTiO_x$ (68.6 μmol/g) > TiO_2 (40.0 μmol/g) ≫ Fe_2O_3 (8.7 μmol/g).

The interaction between iron and titanium species in $FeTiO_x$ resulted in larger amount of Brønsted acid sites per weight than those on pure TiO_2 and Fe_2O_3, which was beneficial to the SCR reaction. This result is in well accordance with the *in situ* DRIFTS of NH_3 adsorption over these three samples (Fig. S1 in Supporting information). After NH_3 adsorption at 30 °C, the bands of NH_4^+ adsorbed on $FeTiO_x$ showed a much higher intensity than those on TiO_2, and the amount of NH_4^+ species detected on Fe_2O_3 was rather small. After normalization by BET surface areas, the NH_3 adsorption amounts on these three samples decreased in the following sequence: TiO_2 (0.39 μmol/m^2) > $FeTiO_x$ (0.28 μmol/m^2) > Fe_2O_3 (0.20 μmol/m^2), indicating that Ti species showed higher NH_3 adsorption ability than Fe species. Based on these results, a model for Brønsted and Lewis acid sites on $FeTiO_x$ catalyst was proposed, as shown in the inset of Fig. 1A. The Brønsted acid sites were mainly composed of acidic hydroxyls linked to Ti^{4+} and sulfate species, while the Lewis acid sites were mainly composed of unsaturated Ti^{4+} and Fe^{3+}. From NH_3 desorption amounts over $FeTiO_x$, TiO_2 and Fe_2O_3, it is concluded that NH_3 mainly adsorbed on titanium sites, but not iron sites of $FeTiO_x$ catalyst in the form of ionic NH_4^+ and coordinated NH_3, which could further participate in the SCR reaction.

Fig. 1B shows the NO_x-TPD profiles over three samples, among which $FeTiO_x$ catalyst had the largest NO_x desorption amount. It was reported that [17] physisorbed NO_x usually desorbed from catalyst surface below 100 °C, and according to this, no physisorbed NO_x was detected over all samples in this study. Both $FeTiO_x$ and Fe_2O_3 had three desorption peaks, whereas TiO_2 only showed two. Comparing with the *in situ* DRIFTS of NO_x desorption over $FeTiO_x$ and Fe_2O_3 (Fig. S2 in Supporting information), the desorption peaks below 150 °C can be ascribed to the decomposition of monodentate nitrate. The desorption peaks centered at 203 °C for $FeTiO_x$ and 324 °C for Fe_2O_3 can be ascribed to the decomposition of bridging nitrate with different thermal stability. The desorption peaks in the high temperature range centered at 320 °C for $FeTiO_x$ and 374 °C for Fe_2O_3 are assigned to the decomposition of bidentate nitrate. For TiO_2, the two desorption peaks at 303 and 356 °C can be assigned to the decomposition of bridging nitrate and bidentate nitrate, respectively.

From NO_x desorption amounts over these three samples, we can see that NO_x could adsorb on both iron sites and titanium sites over $FeTiO_x$ catalyst. However, previous study [5] showed that NO_x could not adsorb on NH_3 pre-covered Ti^{4+} sites due to the greater basicity of NH_3. Considering the NH_3-TPD results which already showed that NH_3 mainly adsorbed on Ti^{4+} sites, it is deduced that under the SCR condition NO_x mainly adsorbed on Fe^{3+} sites in the form of monodentate nitrate or bidentate nitrate, rather than bridging nitrate between Fe^{3+} and Ti^{4+} sites because of the blockage of Ti^{4+} sites in Fe–O–Ti structure by adsorbed NH_3 species. Subsequent TPSR and *in situ* DRIFTS study will reveal what kinds of nitrate species can finally be transformed into N_2 in the SCR condition.

3.2. TPSR experiments

Fig. 2A shows the results of TPSR between NO and pre-adsorbed NH_3 species over $FeTiO_x$. Below 100 °C, NH_3 and H_2O desorption was significant and NO concentration showed no decrease, which meant that the SCR reaction did not occur. The N_2 and N_2O formation below 100 °C might be attributed to the decomposition of some surface nitrogenous species, which were formed through the reaction between NO_x and adsorbed NH_3 species in presence of H_2O at room temperature [17]. Above 100 °C, NO concentration had a steady decrease, implying the occurrence of SCR reaction, and the minimum NO concentration was obtained from 200 to 350 °C. In this temperature range, both N_2 and H_2O had a broad band above baseline and no N_2O formation was observed, suggesting that the selectivity to N_2 was rather high. Above 350 °C, the pre-stored NH_3 species on the catalyst surface seemed to be totally consumed, resulting in the increase of NO and simultaneous decrease of N_2 in gas phase. This TPSR result showed that NO could react with

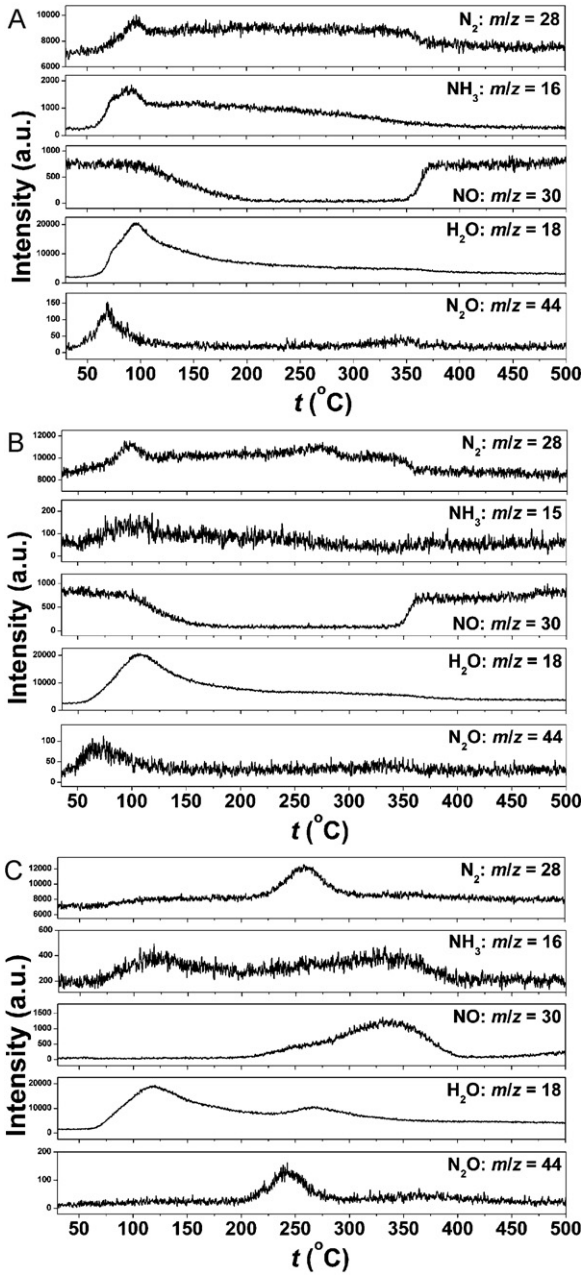

Fig. 2. TPSR profiles of (A) NO with adsorbed NH_3 species, (B) NO + O_2 with adsorbed NH_3 species, and (C) NH_3 with adsorbed NO_x species over $FeTiO_x$.

adsorbed NH_3 species in the absence of O_2 to form N_2 and H_2O, and the lattice oxygen in $FeTiO_x$ catalyst might be involved in the SCR reaction, which is in well accordance with our previous conclusion [2].

To further investigate the effect of O_2 in the SCR reaction, TPSR between NO + O_2 and pre-adsorbed NH_3 species was also conducted (Fig. 2B). In contrast to that with NO only in Fig. 2A, NO was consumed more rapidly to the minimum concentration at 150 °C in the presence of O_2. An enlarged operation temperature window was thus obtained. This result showed that O_2 played an important role in the promotion of SCR reaction, especially in the low temperature range where the NO oxidation by O_2 was significant. The TPSR results with and without O_2 also implied in an opposite side that NO could participate in the SCR reaction in gaseous or weakly adsorbed phase at relatively high temperatures (>200 °C) without undergoing the oxidation step by gaseous O_2.

Moreover, TPSR experiment between NH_3 and pre-adsorbed NO_x species was conducted (Fig. 2C). With the increase of reaction temperature, both NH_3 and H_2O firstly had a desorption band around 150 °C, and then NH_3 had an obvious consumption from 200 to 250 °C. This NH_3 consumption was due to the occurrence of SCR reaction because both N_2 and H_2O had an evident formation peak centered at *ca.* 250 °C. A small amount of N_2O was also detected in this temperature range, implying that the pre-adsorbed nitrogenous species did not totally convert into N_2 through the reaction with NH_3. Afterwards, a slight increase of NO was observed at about 250 °C, which was caused by the decomposition of some bridging nitrate. Above 300 °C, a large amount of NH_3 and NO desorbed from the catalyst surface, and both of the N_2 and H_2O concentrations returned to the baselines. Comparing with the NO_x-TPD results, this NO_x desorption peak was mainly caused by the decomposition of bidentate nitrate which had the highest thermal stability over $FeTiO_x$ catalyst. This result showed that bidentate nitrate was not reactive in the SCR reaction, just as the spectator species. The same phenomenon was also observed in previous studies [18–21], in which bidentate nitrate was not or less reactive in the SCR reaction towards various reducing agents (NH_3, C_3H_6 or C_3H_8). This conclusion will also be verified in the following *in situ* DRIFTS study.

3.3. TR experiments

To further elucidate the SCR reaction pathways over $FeTiO_x$ catalyst, we also conducted TR experiments at fixed temperatures (200 °C and lower 150 °C). Fig. 3A shows the results of NH_3 pulse reaction with pre-adsorbed NO_x species at 200 °C, in which the arrowheads indicate the on–off of NH_3. After the first NH_3 pulse, only a small amount of N_2 was produced due to the reaction between NH_3 and surface nitrate species. H_2O formation was not observed because its amount was too small to be detected. After the second NH_3 pulse, neither N_2 nor H_2O was detected, implying that the reactive nitrate species was completely consumed in the first pulse. During the whole process, the concentration of NH_3 in gas phase did not change due to its strong adsorption onto the catalyst surface. These results show that at this temperature (200 °C), some nitrate species indeed could react with NH_3 species to form N_2 following the L–H mechanism, but the amount was rather small under the reaction condition we set. However, in the real SCR condition at relatively low temperatures (<200 °C), continuous formation of reactive nitrate species on iron sites in the presence of gaseous NO + O_2 could occur due to its rapid reduction by adsorbed NH_3 species. In order to further confirm this short conclusion, we also carried out a similar TR experiment at 150 °C, at which more reactive nitrate species could form on the catalyst surface. As shown in Fig. 3C, more N_2 resulting from the surface reaction between reactive nitrate species and adsorbed NH_3 species was clearly observed after the five NH_3 pulses. These results indicate that the L–H reaction pathway over $FeTiO_x$ catalyst indeed contributed to the overall SCR reaction, especially at temperatures below 200 °C.

For comparison, we also carried out TR experiment of NO + O_2 pulse reaction with pre-adsorbed NH_3 species at 200 °C (Fig. 3B). The arrowheads indicate the on–off of NO + O_2 simultaneously. Being different from the results in Fig. 3A, in the total six NO + O_2 pulses, both N_2 and H_2O immediately formed, implying that the NO_x in gas phase or in weakly adsorbed state could react with adsorbed NH_3 species rapidly, following an E–R mechanism. After the six pulses, NO + O_2 was kept open all the time to consume the residual adsorbed NH_3 species. After nearly 130 min, a breakthrough curve of NO with a steady increase in concentration was obtained. At the same time, both N_2 and H_2O had a steady decrease. As the similar TR experiment at 150 °C shown in Fig. 3D, it only took *ca.* 70 min to obtain the breakthrough curve of NO, indicating that the E–R reaction pathway was relatively weakened to a certain

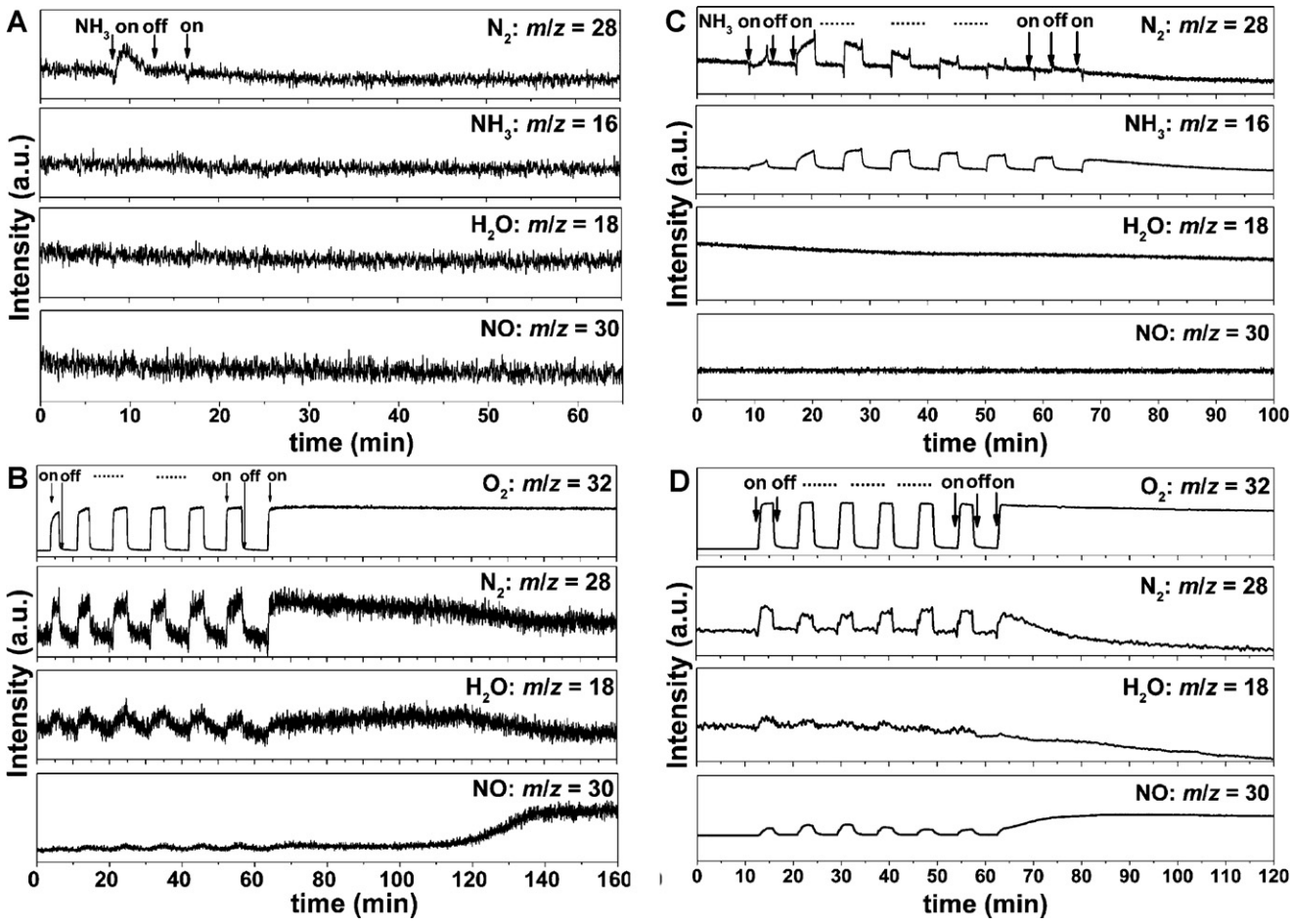

Fig. 3. TR profiles of NH_3 pulse reaction with adsorbed NO_x species at (A) 200 °C and (C) 150 °C, and $NO + O_2$ pulse reaction with adsorbed NH_3 species at (B) 200 °C and (D) 150 °C over $FeTiO_x$ catalyst.

extent at lower reaction temperatures below 200 °C. Summarizing the TR results, it is concluded that both of the reaction pathways including L–H mechanism and E–R mechanism were involved in the SCR process, as further confirmed by the following *in situ* DRIFTS results.

3.4. *In situ DRIFTS experiments*

Fig. 4A shows the *in situ* DRIFTS of reaction between NH_3 and pre-adsorbed NO_x species over $FeTiO_x$. After $NO + O_2$ adsorption and N_2 purge, the catalyst surface was mainly covered by nitrate species. Two hydroxyl consumption bands at 3732 and 3691 cm^{-1} due to the interaction between basic OH and NO_x (mainly NO_2) [22] were observed. Bands at 1556 (ν_3 high) and 1578 (ν_3 high) cm^{-1} can be ascribed to monodentate nitrate and bidentate nitrate, respectively [18,20,23]. The assignments of the band near 1616 cm^{-1} were diverse in previous studies by other researchers [18,20,24,25]. Long and Yang [6] assigned this band to adsorbed NO_2 species (nitro or adsorbed NO_2 molecule) due to its different thermal stability from those of other nitrate species. However, in this study we found that both of the bands at 1616 (ν_3 high) and 1201 (ν_3 low) cm^{-1} should be ascribed to bridging nitrate [23,26], because these two bands showed the same thermal stability in the *in situ* DRIFTS results of NO_x desorption (Fig. S2 in Supporting information) and same reactivity in the following reaction process.

After NH_3 introduction for 1 min, the bands of monodentate nitrate and bridging nitrate immediately moved to lower wave numbers (1552 and 1610 cm^{-1}), implying the decrease of surface coverage because of the reduction by NH_3. At the same time, NH_3 strongly adsorbed onto the surface and the band at 1209 cm^{-1} [27] attributed to coordinated NH_3 (δ_s) bound to Lewis acid sites might have overlapped with the shifted band of bridging nitrate at low wave numbers (1201 cm^{-1}). After 5 min, both of the monodentate nitrate and bridging nitrate disappeared and only bidentate nitrate at 1578 cm^{-1} remained on the surface, implying that bidentate nitrate was indeed inactive in the SCR reaction. Meanwhile, the IR bands attributed to coordinated NH_3 (δ_{as} at 1603 cm^{-1} and δ_s at 1209 cm^{-1}) continued growing, and the bands in the region of 3400–3100 cm^{-1} attributed to N–H stretching vibration in coordinated NH_3 were also observed [28]. Noticeably, a small band at 1529 cm^{-1} ascribed to NH_2 (scissoring vibration mode) from H-abstraction of coordinated NH_3 also occurred [26,29], which was an important intermediate species to react with NO to produce nitrosamine (NH_2NO) and then to decompose into N_2 and H_2O. NH_4^+ bound to Brønsted acid sites (δ_s at 1684 cm^{-1} and δ_{as} at 1437 cm^{-1}) was also formed [30]. Interestingly, an intense negative band at 1364 cm^{-1} ($\nu_{as\,OSO}$) showed up, which is caused by the reaction between NH_3 and sulfate species to form NH_4^+. This negative band proves the existence of residual sulfate species on catalyst surface, and it can also be used as an indicator for the existence of NH_4^+. Comparing with the spectrum after $NO + O_2$ adsorption and N_2 purge, the two hydroxyl consumption bands moved to 3693 and 3655 cm^{-1}, which proved again that the adsorption sites of NH_3 on $FeTiO_x$ catalyst were different from those of NO_x.

Fig. 4B shows the *in situ* DRIFTS of reaction between $NO + O_2$ and pre-adsorbed NH_3 species. After NH_3 adsorption and N_2 purge, the

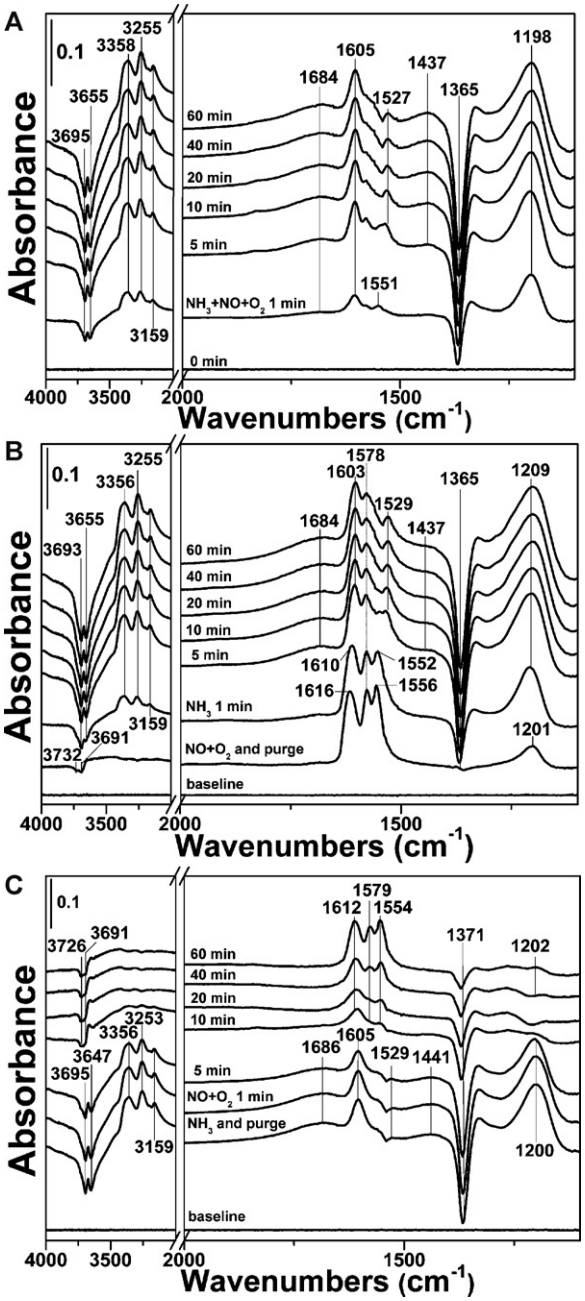

Fig. 4. *In situ* DRIFTS of reaction between (A) NH_3 and adsorbed NO_x species, (B) $NO + O_2$ and adsorbed NH_3 species, and (C) $NH_3 + NO + O_2$ (SCR condition) over $FeTiO_x$ at 200 °C.

bands belonging to coordinated NH_3 (δ_{as} at 1605 cm^{-1} and δ_s at 1200 cm^{-1}) and ionic NH_4^+ (δ_s at 1686 cm^{-1} and δ_{as} at 1441 cm^{-1}) appeared. Negative band at 1371 cm^{-1}, NH_2 band at 1529 cm^{-1}, N–H stretching vibration in the region of 3400–3100 cm^{-1} together with two hydroxyl consumption bands at 3695 and 3647 cm^{-1} also showed up.

After $NO + O_2$ introduction for 5 min, no formation of nitrate species was observed, whereas the band intensity of coordinated NH_3 had an obvious decrease. A slight decrease of band intensity of ionic NH_4^+ was also observed, which was associated with the partial recovery of hydroxyl consumption bands and negative band at 1371 cm^{-1}. This result implied that under this reaction condition both of coordinated NH_3 and ionic NH_4^+ could react with $NO + O_2$, and the reaction between coordinated NH_3 and NO dominated following an E–R mechanism. After 10 min, coordinated NH_3 species were consumed completely and nitrate species began to form on the surface. At the same time, ionic NH_4^+ continued to be consumed with a faster speed that could be judged from the recovery of the negative band at 1371 cm^{-1}. This meant that ionic NH_4^+ favored the reaction with nitrate species following an L–H mechanism. After 60 min, the surface was mainly covered by nitrate species which contained bridging nitrate at 1612 and 1202 cm^{-1}, bidentate nitrate at 1579 cm^{-1} and monodentate nitrate at 1554 cm^{-1}. The increase of bridging nitrate associating with the decrease of adsorbed NH_3 species proved the deduction that only after the titanium site in Fe–O–Ti structure occupied by NH_3 was liberated, bridging nitrate could form on catalyst surface.

Finally, the evolution of surface species over $FeTiO_x$ catalyst in the real SCR condition was investigated (Fig. 4C). After $NH_3 + NO + O_2$ introduction for 1 min, besides of the adsorbed NH_3 species occurred on catalyst surface, a small amount of monodentate nitrate was also detected, which could further react with ionic NH_4^+ to form N_2. From 5 to 60 min, no nitrate species was present on the surface and only adsorbed NH_3 species were observed. NH_2 species after H-abstraction of coordinated NH_3 also showed up at 1527 cm^{-1}. This result suggested that the reaction between NH_4^+ and monodentate nitrate or between NH_2 and NO was very fast.

4. Discussion

4.1. SCR mechanism in the low temperature range

NH_3-TPD results in Section 3.1 combined with the *in situ* DRIFTS of NH_3 desorption in Fig. S1 have already revealed that both Brønsted and Lewis acid sites existed on the surface of $FeTiO_x$ catalyst. Long et al. [6,31] reported that there were a larger proportion of Brønsted acid sites than Lewis acid sites at low temperatures on Fe^{3+}–TiO_2–PILC catalyst, which is consistent with our results. As we described in Section 3.1, NH_3 mainly adsorbed on titanium sites of $FeTiO_x$ catalyst in the form of ionic NH_4^+ and coordinated NH_3. However, the coordinated NH_3 showed less reactivity in the low temperature range because of its higher activation energy to form NH_2 species [32]. Therefore, NH_4^+ was the main reactive adsorbed NH_3 species in the SCR condition below 200 °C.

Furthermore, NO was easy to be oxidized by O_2 over Fe^{3+} [7] and then further adsorb onto the iron sites to form nitrate species (mainly monodentate nitrate in the SCR condition as we described in Sections 3.1 and 3.4). Over the $FeTiO_x$ catalyst at low temperatures, the reactive monodentate nitrate on iron sites could react with two neighboring NH_4^+ on titanium sites to form intermediate species, which could further react with gaseous or weakly adsorbed NO to form N_2 [33,34]. Thereupon, we can propose an L–H mechanism dominant for the SCR reaction over $FeTiO_x$ catalyst in the relatively low temperature range (<200 °C), as shown in Fig. 5A. In this mechanism, gaseous O_2 played an important role in NO oxidation. The overall reaction after the formation of intermediate species is as follows: $2NH_4^+ + NO_2\,(ads) + NO \rightarrow 2\,N_2 + 3H_2O + 2H^+$, which is exactly the "fast SCR" mechanism proposed by other researchers [35,36]. This explains the reason for the significant enhancement in the low temperature SCR activity over $FeTiO_x$ catalyst when the NO_2/NO molar ratio was adjusted to 1:1 in our previous study [2]. Under the SCR condition, as the *in situ* DRIFTS results shown, only adsorbed NH_3 species was detected on the surface, implying that once the active monodentate nitrate was formed, it could be consumed quickly to produce the final products. Therefore, the formation of monodentate nitrate on iron sites was actually the rate-determining step for the overall SCR reaction.

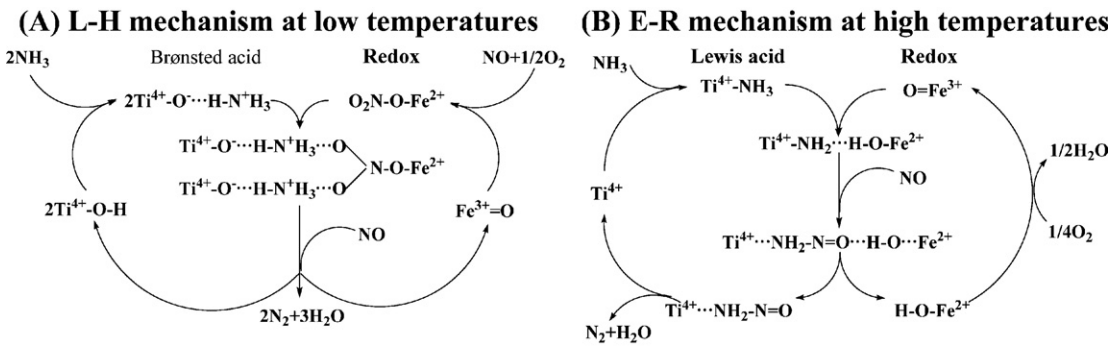

Fig. 5. Proposed SCR mechanisms over $FeTiO_x$ catalyst in different temperature ranges.

4.2. SCR mechanism in the high temperature range

At relatively high temperatures (>200 °C), some Brønsted acid sites could be transformed into Lewis acid sites due to the dehydroxylation and dehydration effect [31]. As the *in situ* DRIFTS results shown in Section 3.4, the coordinated NH_3 adsorbed on titanium sites could further undergo oxidative dehydrogenation by neighboring Fe^{3+} to form NH_2 intermediate species. Moreover, as the TPSR results shown in Section 3.2, NO could react with NH_2 species directly to form NH_2NO intermediate species without oxidation by O_2. Because of the low thermal stability and rapid decomposition of NH_2NO into N_2 and H_2O, no infrared band attributed to NH_2NO was observed on catalyst surface under the SCR condition. Therefore, the formation of NH_2NO was actually the rate-determining step in the overall SCR reaction. During this process, Fe^{3+} was firstly reduced to Fe^{2+} in the H-abstraction step of coordinated NH_3, and then reoxidized to Fe^{3+} by O_2 to complete a redox circle. Accordingly, we can propose an E–R mechanism for the SCR reaction over $FeTiO_x$ catalyst as shown in Fig. 5B, which is mainly predominant in the high temperature range (>200 °C). The similar SCR reaction pathway was also proposed on V_2O_5–WO_3/TiO_2 [29], MnO_x–CeO_2 [37] and Fe_2O_3–WO_3/ZrO_2 [8] catalysts by other researchers.

4.3. Enlightenment

The comprehensive understanding of NH_3-SCR mechanisms in different temperature ranges can supply theoretical guidance for the catalyst redesign and activity improvement for environmental-friendly $FeTiO_x$ catalyst, even for other Fe-based SCR catalysts. To further enhance the low temperature $DeNO_x$ efficiency, the L–H reaction pathway between ionic NH_4^+ and monodentate nitrate at low temperatures should be strengthened. Therefore, for $FeTiO_x$ SCR catalyst of which the NH_3 adsorption ability is already strong enough, a wise method is to increase its NO oxidation ability and thus to increase the formation of reactive monodentate nitrate. A good example is to substitute partial Fe in $FeTiO_x$ catalyst by Mn with higher oxidative ability, through which the formation of monodentate nitrate is largely enhanced and the low temperature $DeNO_x$ efficiency is also obviously improved [38].

In our previous study, it has been concluded that even over the SO_2-posioned $FeTiO_x$ catalyst, the NO_x conversion still could be maintained above 90% from 250 to 400 °C [1]. This is mainly owing to the mechanistic nature of E–R reaction pathway between NH_2 species and NO at high temperatures, on which the deposited sulfate species showed no inhibition effect at all.

It is optimal for us to find a certain SCR catalyst, over which the NH_3-SCR reaction follows an E–R mechanism between NH_2 and NO at low temperatures, or the sulfate species could decompose readily at low temperatures on the catalyst surface, thus we can obtain high $DeNO_x$ efficiency and high SO_2 durability simultaneously even below 100 °C. This can be a struggling aim for $DeNO_x$ researchers, although there is still a long journey to conquer.

5. Conclusions

Both Brønsted acid sites and Lewis acid sites existed on the surface of iron titanate catalyst $FeTiO_x$. During the SCR process, NH_3 mainly adsorbed onto the titanium sites in a form of ionic NH_4^+ and coordinated NH_3, while NO_x mainly adsorbed onto the iron sites in a form of monodentate nitrate species.

In the low temperature range (<200 °C), the reactive surface species were mainly NH_4^+ and monodentate nitrate, and the SCR reaction mainly followed the L–H mechanism, during which the formation of monodentate nitrate species resulting from the NO oxidation by O_2 over Fe^{3+} sites was the rate-determining step.

In the high temperature range (>200 °C), the reactive surface species were mainly NH_2, and the SCR reaction mainly followed the E–R mechanism, during which the formation of NH_2NO intermediate species after H-abstraction of NH_3 by neighboring Fe^{3+} sites was the rate-determining step. O_2 took effect in the reoxidation of Fe^{2+} (produced in the H-abstraction step) to Fe^{3+} to complete a redox cycle.

Acknowledgements

This work was supported by the National Natural Science Foundation of China (50921064), the Ministry of Science and Technology, China (2009AA064802, 2009AA06Z301) and the Special Co-construction Project of Beijing Municipal Commission of Education.

Appendix A. Supplementary data

Supplementary data associated with this article can be found, in the online version, at doi:10.1016/j.cattod.2011.02.049.

References

[1] F. Liu, H. He, C. Zhang, Chem. Commun. (2008) 2043.
[2] F. Liu, H. He, C. Zhang, Z. Feng, L. Zheng, Y. Xie, T. Hu, Appl. Catal. B: Environ. 96 (2010) 408.
[3] F. Liu, H. He, J. Phys. Chem. C 114 (2010) 16929.
[4] F. Liu, K. Asakura, H. He, Y. Liu, W. Shan, X. Shi, C. Zhang, Catal. Today 164 (2011) 488.
[5] G. Busca, L. Lietti, G. Ramis, F. Berti, Appl. Catal. B: Environ. 18 (1998) 1.
[6] R.Q. Long, R.T. Yang, J. Catal. 190 (2000) 22.
[7] R.Q. Long, R.T. Yang, J. Catal. 207 (2002) 224.
[8] N. Apostolescu, B. Geiger, K. Hizbullah, M.T. Jan, S. Kureti, D. Reichert, F. Schott, W. Weisweiler, Appl. Catal. B: Environ. 62 (2006) 104.
[9] R.Q. Long, R.T. Yang, J. Am. Chem. Soc. 121 (1999) 5595.
[10] R.Q. Long, R.T. Yang, J. Catal. 186 (1999) 254.
[11] P. Balle, B. Geiger, S. Kureti, Appl. Catal. B: Environ. 85 (2009) 109.
[12] M. Iwasaki, K. Yamazaki, K. Banno, H. Shinjoh, J. Catal. 260 (2008) 205.

[13] J.-H. Park, H.J. Park, J.H. Baik, I.S. Nam, C.-H. Shin, J.-H. Lee, B.K. Cho, S.H. Oh, J. Catal. 240 (2006) 47.
[14] L.S. Cheng, R.T. Yang, N. Chen, J. Catal. 164 (1996) 70.
[15] R.Q. Long, R.T. Yang, J. Catal. 207 (2002) 158.
[16] L. Chmielarz, R. Dziembaj, T. Grzybek, J. Klinik, T. Łojewski, D. Olszewska, A. Węgrzyn, Catal. Lett. 70 (2000) 51.
[17] R.Q. Long, R.T. Yang, J. Catal. 198 (2001) 20.
[18] Z. Liu, P.J. Millington, J.E. Bailie, R.R. Rajaram, J.A. Anderson, Micropor. Mesopor. Mater. 104 (2007) 159.
[19] K.I. Shimizu, J. Shibata, A. Satsuma, J. Catal. 239 (2006) 402.
[20] W.S. Kijlstra, D.S. Brands, H.I. Smit, E.K. Poels, A. Bliek, J. Catal. 171 (1997) 219.
[21] Z. Liu, K.S. Oh, S.I. Woo, Catal. Lett. 120 (2008) 143.
[22] G. Piazzesi, M. Elsener, O. Kröcher, A. Wokaun, Appl. Catal. B: Environ. 65 (2006) 169.
[23] G.M. Underwood, T.M. Miller, V.H. Grassian, J. Phys. Chem. A 103 (1999) 6184.
[24] D.A. Peña, B.S. Uphade, E.P. Reddy, P.G. Smirniotis, J. Phys. Chem. B 108 (2004) 9927.
[25] H.Y. Chen, T. Voskoboinikov, W.M.H. Sachtler, J. Catal. 180 (1998) 171.
[26] W.S. Kijlstra, D.S. Brands, E.K. Poels, A. Bliek, J. Catal. 171 (1997) 208.
[27] G. Ramis, M.A. Larrubia, G. Busca, Top. Catal. 11–12 (2000) 161.
[28] G. Busca, M.A. Larrubia, L. Arrighi, G. Ramis, Catal. Today 107–108 (2005) 139.
[29] L. Lietti, G. Ramis, F. Berti, G. Toledo, D. Robba, G. Busca, P. Forzatti, Catal. Today 42 (1998) 101.
[30] N.Y. Topsøe, Science 265 (1994) 1217.
[31] R.Q. Long, M.T. Chang, R.T. Yang, Appl. Catal. B: Environ. 33 (2001) 97.
[32] G. Qi, R.T. Yang, J. Phys. Chem. B 108 (2004) 15738.
[33] V. Sanchez-Escribano, T. Montanari, G. Busca, Appl. Catal. B: Environ. 58 (2005) 19.
[34] J. Li, R. Zhu, Y. Cheng, C.K. Lambert, R.T. Yang, Environ. Sci. Technol. 44 (2010) 1799.
[35] A. Grossale, I. Nova, E. Tronconi, D. Chatterjee, M. Weibel, J. Catal. 256 (2008) 312.
[36] M. Devadas, O. Kröcher, M. Elsener, A. Wokaun, N. Söger, M. Pfeifer, Y. Demel, L. Mussmann, Appl. Catal. B: Environ. 67 (2006) 187.
[37] F. Eigenmann, M. Maciejewski, A. Baiker, Appl. Catal. B: Environ. 62 (2006) 311.
[38] F. Liu, H. He, Y. Ding, C. Zhang, Appl. Catal. B: Environ. 93 (2009) 194.